The Propagation of Shock Waves around Obstacles and in Bent Ducts

LUCIAN Z. DUMITRESCU

Head, Shock-tube Laboratory, Institute of Fluid Mechanics, Bucharest

SUMMARY

The interaction of weak shocks with two-dimensional obstacles, and their propagation in bent ducts, is discussed. Pictures obtained in a shock-tube give support to assumptions, enabling an approximative theory to be developed; pressure recordings agree with computations. Main results are: (*i*) peak transient pressures are double the shock over-pressure; (*ii*) the wave diffraction has a much shorter time-scale than the turbulent wake formation and, therefore, these two processes can be studied independently; (*iii*) the reshaping of the shock after passing through a sharp 90° bend needs about 10 duct diameters and less for rounded bends.

1. INTRODUCTION

The subject of this paper is the propagation of weak shock waves (shock Mach number less than about 1·25, pressure ratio less than about 1·6) around obstacles placed in an indefinite medium, as well as in closed ducts having bends and/or cross-sectional changes. These phenomena share in common many features and the same theoretical arguments will be shown to hold for them.

Aside from the academic interest of these topics, the reason for their investigation lies also in the variety of practical circumstances in which they are encountered: supersonic booms, blasts in mine galleries, transient phenomena in pneumatic control systems and gas pipe-lines, waves produced in the inlet and exhaust manifolds of internal-combustion engines and so on.

Some of the results discussed here have been reported elsewhere[1]; other theoretical works have been published on related topics[2,3,4]; however, no

complete solution has been given yet, nor have published experimental data been found.

This work has been done in the shock-tube laboratory of the Institute of Fluid Mechanics; in Fig. 1 a general view of the laboratory is given, showing one of its shock-tubes in which part of the tests reported here have been carried out. A description of the shock-tube and its performance may be found in ref. 5.

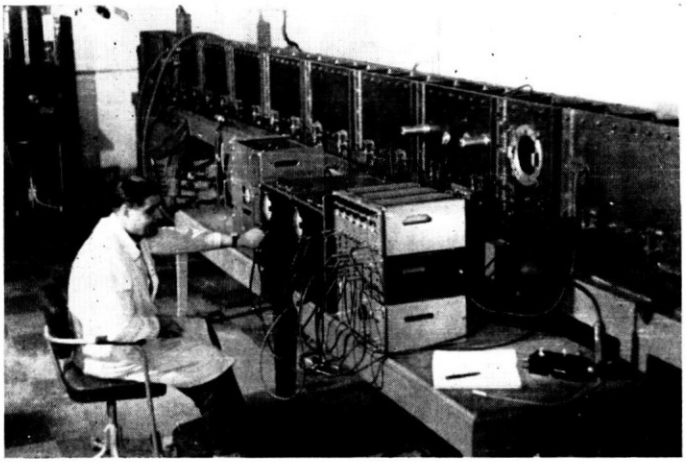

FIG. 1 — General view of the 200 by 300 mm shock-tube

LIST OF SYMBOLS

M_s	incident shock wave propagation Mach number
M_s'	reflected shock wave propagation Mach number
T_1	characteristic time of wave-propagation process
T_2	characteristic time of wave-development process
H	characteristic dimension of the obstacle
t	time
a	velocity of sound
u, v	flow velocity components
p	pressure
ρ	density
x, y	co-ordinates in the physical plane
$\bar{x}, \bar{y}; X, Y$	transformed co-ordinates
r, θ	polar co-ordinates in plane $(\bar{x}, \bar{y})$
R, ϕ	polar co-ordinates in plane (X, Y)

$Z = X + iY$ complex variable
$\zeta = \xi + i\eta$ transformed complex variable
$\ln x$ natural logarithm function
Δ Laplace operator

2. Qualitative Discussion

The basic configuration showing the essential features of the diffraction process may be seen in Fig. 2(*a*). This is a shadowgraph of the wave pattern produced by a shock wave which strikes a blunt two-dimensional obstacle. A diagrammatic sketch of the picture is given in Fig. 2(*b*). It can be seen that

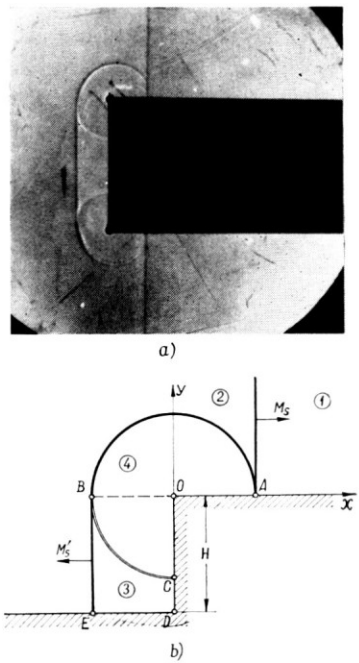

Fig. 2 (*a*), (*b*) — The diffraction of a shock wave around a blunt obstacle

the incident shock wave, M_s, is reflected from the body as from a solid wall, and a reflected shock, M_s', is formed. The presence of the corner O produces a disturbance which propagates itself as a quasi-circular wave ABC. As the incident shock is weak, all propagation velocities do not differ much from the sound speed.

Therefore, in Fig. 2(*b*), the perturbed region has been drawn as truly circular. Its boundary is formed by a rarefaction wave, *BC*, which propagates into the stagnation region *3*, left behind by the reflected shock, and a compression wave, *AB*, propagating into the uniform flow *2*, behind the incident shock.

From the practical standpoint, it is the pressure distribution on the obstacle walls that presents interest; therefore, the slight distortion of the actual wave pattern introduced by assuming all wave speeds to be equal should be of little consequence.

Finally, in Fig. 2(*a*) one may see a vortex taking shape at the corner of the model.

In the later stages of the motion, the disturbances originated at the opposite corners of the obstacle (or reflected from the lower wall) will overlap; the successive configurations are shown in Figs. 3(*a*), (*b*), (*c*). Subsequently, other disturbances are produced at the corners and the wave pattern becomes more complex; however, the intensity of the perturbations diminishes gradually and eventually a quasi-steady flow regime is reached, governed by the equations of incompressible steady flows. Other flow pictures, not reproduced here, show that the corner vortex breaks down rather late in the process.

The second basic configuration is the reverse of the first (Fig. 4(*a*), (*b*)). The

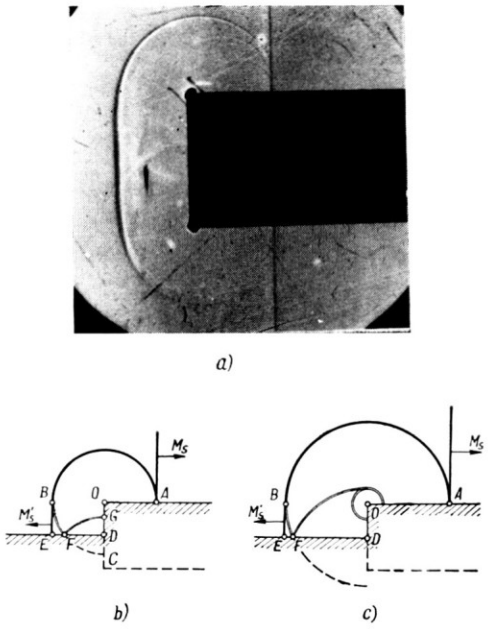

FIG. 3 (*a*), (*b*), (*c*) — The evolution of the diffraction process

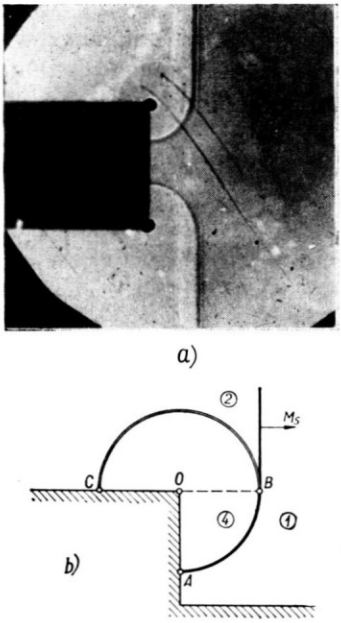

FIG. 4 (*a*), (*b*) — The expansion of a shock wave over a step

FIG. 5 — The breakdown of the corner vortex

evaluation of this motion is somewhat more difficult, since the wave diffraction process takes place in the same region where the turbulent wake will ultimately develop and it is not clear *a priori* how these two phenomena will interact. The experimental evidence suggests that the wave propagation process is more or less independent of the wake formation; therefore, it has been concluded that these two processes can be studied separately. In Fig. 5 one may see how the corner vortex breaks down and is drawn away with the flow speed.†

The independence of the two processes can also be justified by a reminder that the wave diffraction is a phenomenon associated to a characteristic time, T_1, related to the propagation velocity of the disturbances (i.e. the speed of sound, a); $T_1 = O(H/a)$, where H is the main dimension of the obstacle. On the other hand, the wake development proceeds with a time-scale T_2, which is related to the mean flow velocity u; $T_2 = O(H/u)$. As, for weak shock waves, u is much smaller than a, the two time-scales are very different and the two processes should not interact significantly.

† These pictures suggest the idea of a study of the rolling-up and breakdown of an attached vortex, using the shock-tube technique, as an independent problem, more connected with boundary-layer research.

In this manner, two simplifying principles have been established for the flows dealt with here: (*i*) that the geometrical pattern of the diffracted waves can be simplified, assuming the same velocity for all waves; and (*ii*), that the two processes discussed above are independent and, in the early stages, the flow may be considered as potential.

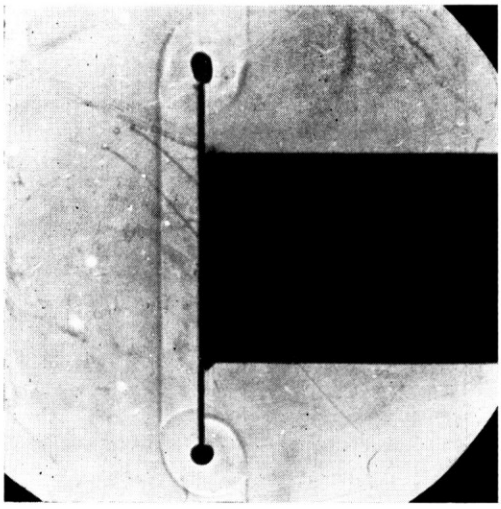

FIG. 6 — The passage of a shock wave over a flat plate

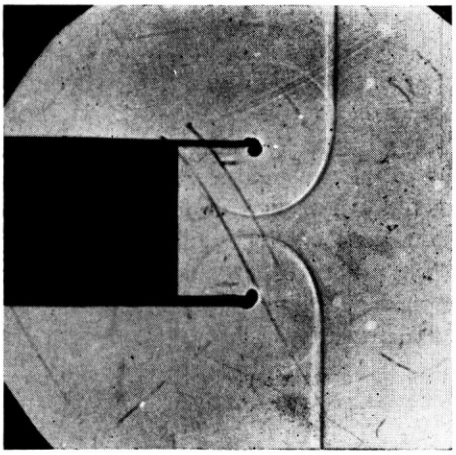

FIG. 7 — Reversal of the flow direction around a plate

These principles greatly simplify the theoretical treatment of the problem, as will be shown later. Further tests have been made to check how far they can be applied. Thus, in Fig. 6, one may see the shock wave striking a flat plate put across the flow; the resultant wave pattern is a combination of those shown in Figs. 2 and 4.

In Fig. 7 one may see that the flow direction can be deflected by a full 180° in the early stages of the process; this establishes beyond doubt the validity of the above mentioned principles.

Other obstacle shapes (wedges, rounded corners and so on) have also been investigated; flow visualisations and theoretical formulae for these are given elsewhere[1].

3. Theoretical Analysis

The analytical treatment of the problem will be discussed briefly, taking the case shown in Fig. 2 as an example; all other configurations can be dealt with easily in the same manner[1].

The flow parameters in regions *1*, *2* and *3* are known; only the motion in the perturbed region *4* has to be determined. The equations of motion are:

$$\frac{\partial u}{\partial t}+u\frac{\partial u}{\partial x}+v\frac{\partial u}{\partial y}=-\frac{1}{\rho}\frac{\partial p}{\partial x} \tag{1}$$

$$\frac{\partial v}{\partial t}+u\frac{\partial v}{\partial x}+v\frac{\partial v}{\partial y}=-\frac{1}{\rho}\frac{\partial p}{\partial y} \tag{2}$$

$$\frac{\partial \rho}{\partial t}+\rho\left(\frac{\partial u}{\partial x}+\frac{\partial v}{\partial y}\right)+u\frac{\partial \rho}{\partial x}+v\frac{\partial \rho}{\partial y}=0 \tag{3}$$

$$\frac{\mathrm{d}p}{\mathrm{d}\rho}=a^2 \tag{4}$$

where u and v are the velocity components in the x and y directions, p the pressure, ρ the density, and a the speed of sound.

According to the principles already established, it can be seen that the flow sketched in Fig. 2(*b*) has no characteristic dimension, so long as the perturbation waves do not overlap, or are reflected by the bottom wall *DE*. Therefore, the motion is self-similar, and the problem can be simplified by the introduction of transformed variables:

$$\bar{x}=x/at, \quad \bar{y}=y/at \tag{5}$$

Furthermore, as the velocities are small, in the transformed equations, higher-order terms, such as $u\,\partial u/\partial x$, can be neglected; thus, after certain transformations, the following equation for the pressure is obtained:

$$\Delta p = \left(\bar{x}\frac{\partial}{\partial \bar{x}} + \bar{y}\frac{\partial}{\partial \bar{y}}\right)\left(\bar{x}\frac{\partial p}{\partial \bar{x}} + \bar{y}\frac{\partial p}{\partial \bar{y}}\right) \tag{6}$$

Following Smyrl[3], this is reduced to the Laplace equation, $\Delta p = 0$, by the use of the Busemann transformation:

$$r = \frac{2R}{1+R^2}, \quad \theta = \phi \tag{7}$$

which maps the plane $(\bar{x}, \bar{y})$, in which polar co-ordinates (r, θ) have been introduced, into the plane (X, Y), of polar co-ordinates (R, ϕ). The domain *4* in Fig. 2(*b*) is mapped inside a circle of unit radius, as shown in Fig. 8(*a*).

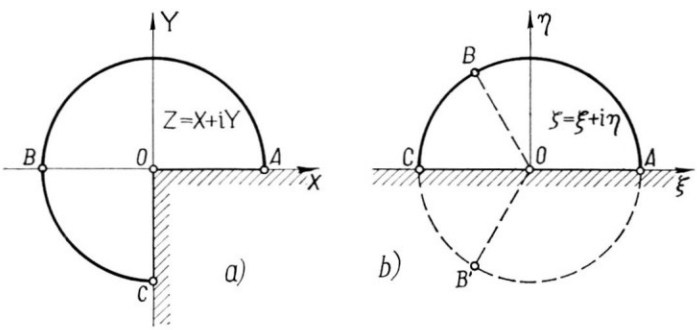

FIG. 8 (*a*), (*b*) — The transformed disturbance domain of Fig. 2 (*b*)

The boundary conditions for the problem are the following:

along AB: $(0 < \phi < \pi)$: $\qquad p = p_2 = \text{const.}$ (8)

along BC: $\left(\pi < \phi < \frac{3\pi}{2}\right)$: $\qquad p = p_3 = \text{const.}$ (9)

along OA: $(\phi = 0)$: $\qquad \frac{\partial p}{\partial \bar{y}} = \frac{\partial p}{\partial \phi} = \frac{\partial p}{\partial Y} = 0$ (10)

along OB: $\left(\phi = \frac{3\pi}{2}\right)$: $\qquad \frac{\partial p}{\partial \bar{x}} = \frac{\partial p}{\partial \phi} = \frac{\partial p}{\partial X} = 0$ (11)

Conditions (10) and (11) are equivalent to that of vanishing normal velocities on the walls, keeping account of the transformations of equations (5) and (7).

To solve the problem, the domain of Fig. 8(*a*) is conformally mapped into a half-circle in the plane $\zeta = \xi + i\eta$ (Fig. 8(*b*)), by the transform:

$$\zeta = Z^{2/3} \quad (Z = X + iY) \tag{12}$$

and the pressure p is taken as the real part of a complex potential $F(\zeta)$, which is readily determined, after prolonging it by symmetry in the lower half-circle:

$$F(\zeta) = p_2 - \frac{p_3 - p_2}{\pi i}\left(\pi i + \ln \frac{\zeta - e^{2\pi i/3}}{\zeta - e^{-2\pi i/3}}\right) \tag{13}$$

This formula permits the computation of the variation in time of the pressure distribution along the obstacle walls, up to the moment when the perturbation wave, *BC*, reflected from the lower wall, *DE*, reaches the respective point. In the later stages of the motion, the pressure variation can still be approximately determined by assuming that the incident and reflected disturbance waves do not interfere with each other while overlapping and by adding their effects.

Explicit formulae for the pressure distribution on various other obstacle configurations have also been developed[1]. This analysis shows that, whatever the obstacle shape, the maximum over-pressure reached is equal to that produced in the stagnation zone behind a reflected shock; for weak shocks, this is about double the over-pressure of the incident wave.

4. Experimental Results

To check the validity of the theoretical considerations, pressure measurements have been made on models placed in the shock-tube. Details on the measuring technique and electronic equipment are given elsewhere[6, 7, 8, 9, 10]. The specially developed capacitive pressure pick-ups are shown in Fig. 9; they have an overall diameter of 8 mm, a rise-time of about 8 microseconds and a sensitivity of 100 millivolts per atmosphere. Their most outstanding feature is, however, their complete insensitivity to parasitic mechanical vibrations, which allows them to be mounted inside the models without any special precautions. As a measure of their performance qualities, in Fig. 10 an oscilloscope recording is shown of the response to a pure pressure step, obtained by placing the pick-up in the end-wall of the shock-tube. The time-marking frequency displayed in the picture is 500 Kc/s; on all following oscilloscope photographs, the time-marking frequency is 100 Kc/s.

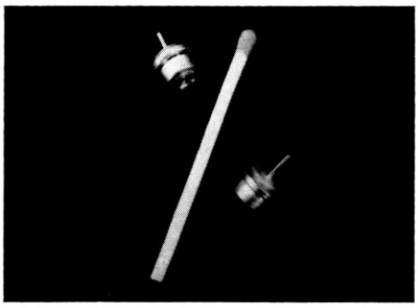

FIG. 9 — A capacitive pressure pick-up

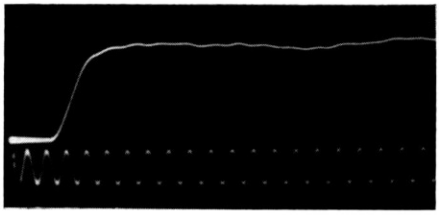

FIG. 10 — The response of the pick-up when mounted in the end-wall of a shock-tube. The time-marking frequency is 500 Kc/s

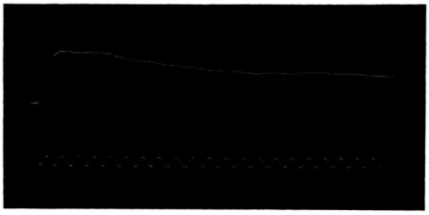

FIG. 11 — The pressure variation at a point on a blunted model. The time-marking frequency is 100 Kc/s

Figure 11 shows the pressure history at a point on the front surface of the blunt model which produced the wave pattern of Fig. 2. In Fig. 12, a comparison is made between the computed pressure variation in time and the actually recorded values, redrawn for the purpose. One may see that the agreement is good, even in the later stages of the motion, when the diffracted waves are interfering with each other. In particular, the predicted value of the maximum over-pressure plateau is obtained.

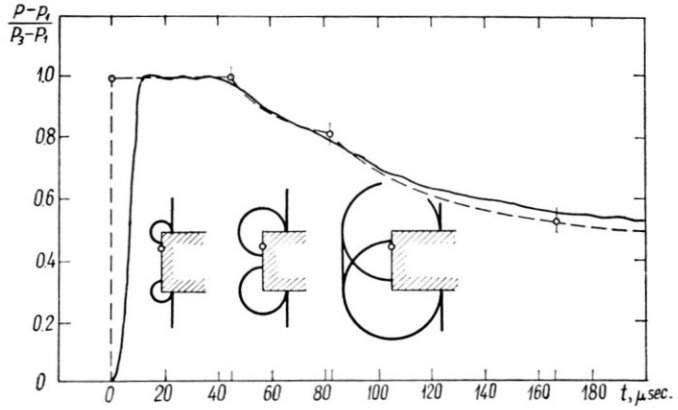

FIG. 12 — Comparison of the theory with experiment for the pressure variation on a blunted model

5. The Propagation of Weak Shock Waves in Bent Ducts

All the foregoing considerations can be applied to the propagation of weak shock waves in bent ducts. For instance, by combining the flow patterns of Figs. 2 and 3, one obtains the picture of the phenomena taking place in a sharp 90° bend. In Fig. 13(*a*) a shadowgraph of the flow is given, obtained in a shock-tube having a 30 mm. square cross-section; Fig. 13(*b*) is a diagrammatic sketch, at the same scale, of the successive wave reflections drawn in accordance with the theoretical agreements developed above. Although the development of the corner vortex begins to interfere with the later reflections, the general features of the flow are still reproduced by the simplified representations.

Figures 14 and 15 show the waves produced in a sharp 45° and a rounded bend, respectively. It may be seen that in the rounded bend the reflected

waves are attenuated very soon and a quasi-normal shock is travelling in the tube.

In connection with these phenomena, two problems of practical interest arise: first, to determine the values of the maximum over-pressures which build up on the tube walls, and second, to establish how the shock wave again takes its normal shape after passing through the bend. In accordance with the arguments developed above, the maximum pressure should be equal

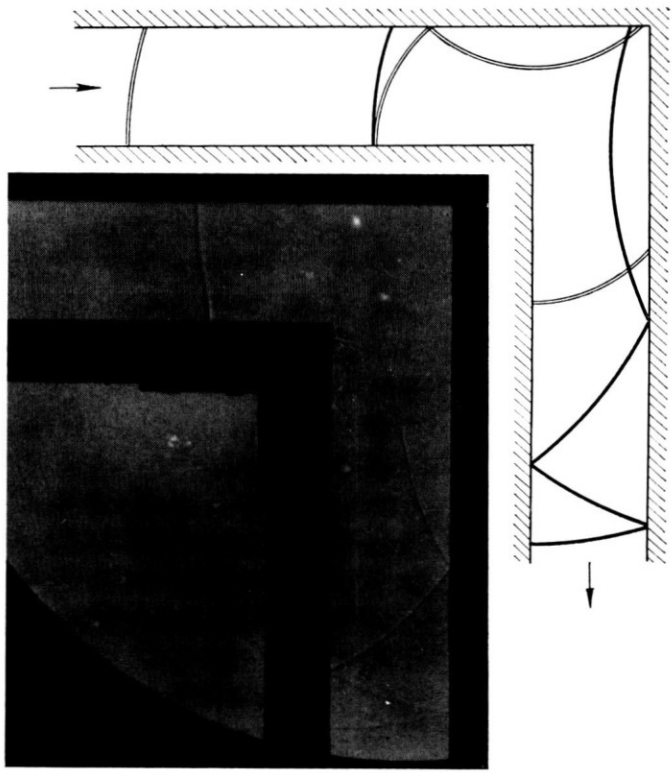

FIG. 13 (*a*), (*b*) — The wave pattern produced by the propagation of a shock wave in a sharp bend

to that behind a reflected normal shock (about double the incident shock strength) and be produced near the corner of sharp bends. This result has been substantiated by experiments.

The mechanism of re-formation of the shock wave involves the overtaking and coalescence of several diffracted waves and cannot be accounted for by

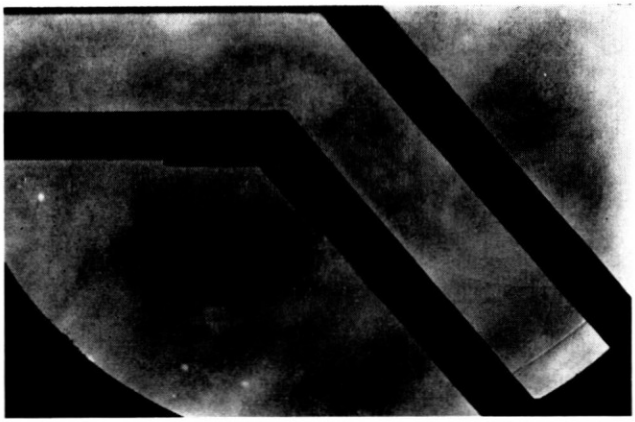

FIG. 14 — The wave system produced by the passage of a shock wave through a 45° bend

the simplified theory, which supposes constant wave velocities; therefore, a series of tests have been made, recording the pressure on an end-wall placed at various distances downstream of the corner of a 90° bend.

Some of the oscilloscope recordings are shown in Figs. 16(*a*), (*b*), (*c*), (*d*); from these tests, it is concluded that, at a distance of about 10 tube widths, the plane shock wave may be considered as re-established. Flow shadowgraphs have confirmed this result, showing a straight shock followed by a sequence of attenuated oblique waves.

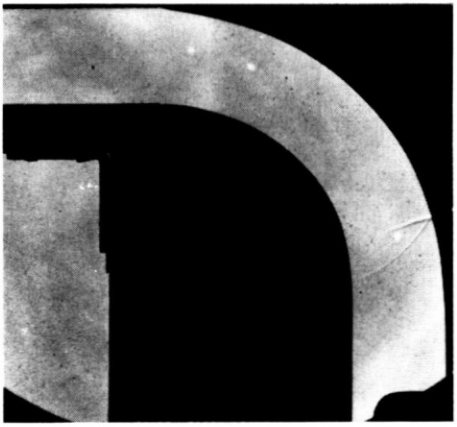

FIG. 15 — The propagation of a shock wave through a rounded 90° bend

For rounded bends, the pressure recordings and the visualisations show that the shock wave is re-shaped almost immediately after emerging from the corner.

This behaviour of the shock waves in sharp and rounded bends may be

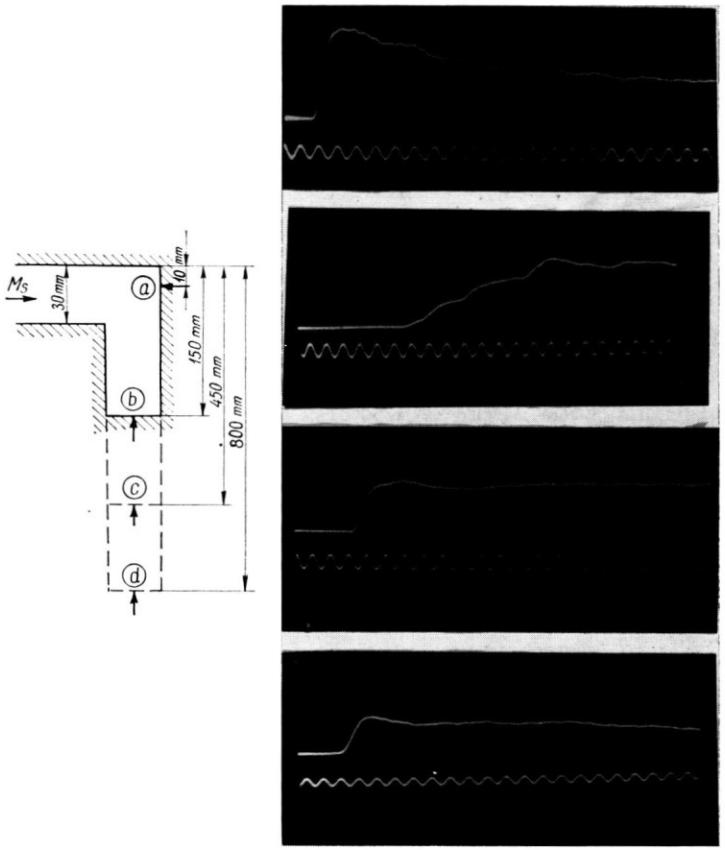

FIG. 16 (*a*), (*b*), (*c*), (*d*) — Oscilloscope recordings of the pressure variation in a sharp bend. The time-marking frequency is 100 Kc/s

paralleled to the way in which uniform velocities are re-established in the cross-section of a duct, in steady subsonic flow, downstream of a bend, inasmuch as sharp corners produce strong flow non-uniformities. However, it should be pointed out that these two phenomena have different causes

(wave diffractions in the first case, and boundary-layer separation in the second).

6. The Propagation of Weak Shock Waves in Ducts with Area Discontinuities

Another configuration frequently encountered in practice is that of ducts having cross-sectional discontinuities (contractions or expansions). The respective flow phenomena are also readily accounted for by the methods developed in this paper and some of the results will be discussed briefly here.

Figure 17 shows the wave systems produced in a contracted tube (contraction ratio 2). It can be seen that the shock wave is re-shaped quite soon, leaving behind a uniform flow region but that a system of reflected waves are propagating upstream. Oscilloscope recordings of the pressure in an end-wall placed at various distances downstream of the throat, also show good agreement with the one-dimensional theory (*see*, e.g., ref. 11) for the transmitted shock strength.

The flow in an expanded tube is shown in Fig. 18. Here the shock wave needs a somewhat longer distance to take again its straight shape, and leaves behind a complicated set of reflected waves; however, they are still well

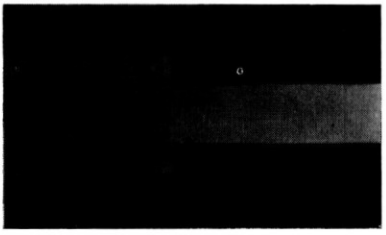

Fig. 17 — The propagation of a shock wave in a contracted duct

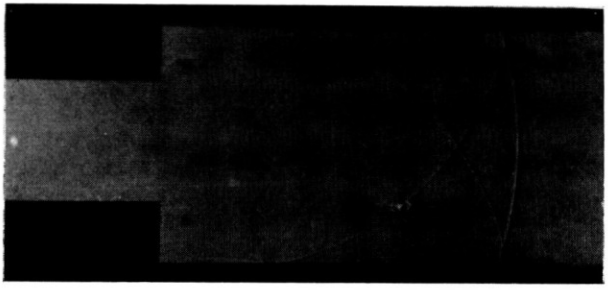

Fig. 18 — The diffraction of a shock wave in an expanded duct

reproduced by the simple theory. The transmitted shock pressure is stabilised to the one-dimensional value only several tube widths downstream; as the theory also predicts, nearer to the throat, end-wall recordings show an initial pressure equal to that produced by the undisturbed shock wave, gradually falling to the value predicted by the one-dimensional theory.

7. Concluding Remarks

Based on experimental evidence, some simplifying arguments have been put forward which allow an approximate theory to be developed for the propagation of weak shock waves around various obstacles, in bent ducts or in tubes with area discontinuities. In particular, the detailed structure of the wave pattern, and the pressure distribution in the early stages of the flow, are well accounted for.

In the future it is hoped to extend this study, on the same lines, to various related problems and in particular to strong shock waves; many interesting phenomena have shown up during the research, giving suggestions for further investigations.

8. Acknowledgments

The continuous guidance and support of Professor E. Carafoli is gratefully acknowledged. The author wishes also to thank his colleagues of the Laboratory for their substantial help in this research.

References

(1) Dumitrescu, Lucian Z., 'The interaction of weak shock waves with obstacles. (I) Development of the unsteady process. (II) Theoretical analysis. (III) Comparison of the theory with experimental results.' To be published in *Revue Roumaine des Sciences Techniques-Mécanique Appliquée.*

(2) Nikolsky, A. A., Smirnov, V. A. 'The action of shock waves on obstacles' (in Russian). *Inzhenernyi Zhurnal*, **2,** 1, 1962.

(3) Smyrl, J. L., 'The impact of a shock wave on a thin two-dimensional airfoil moving at supersonic speed.' *Journal of Fluid Mechanics*, **15,** 2, 1963.

(4) Butler, T. D., 'Numerical calculations of the transient loading of blunt obstacles by shocks in air.' *A.I.A.A. Journal*, **4,** 3, 1966.

(5) Dumitrescu, Lucian Z., 'A shock-tube for aerodynamic research' (in Romanian). *Studii si Cercetări de Mecanică Aplicată* (Bucharest), **10,** 1, 1959.

(6) Procopovici, E. and Dumitrescu L., '*Measurement of aerodynamic pressures in a shock-tube* (in Romanian). *Studii si Cercetări de Mecanică Aplicată* (Bucharest), **12,** 1, 1961.

(7) JAKAB, I., ZAHARESCU, A., DUMITRESCU, L., 'A method for the measurement of the propagation velocity of shock waves' (in Russian). *Revue de Mécanique Appliquée* (Bucharest), **7**, 1, 1962.
(8) DUMITRESCU, LUCIAN Z., 'A method for the dynamic calibration of pressure transducers.' *Revue Roumaine des Sciences Techniques-Mécanique Appliquée*, **9**, 2, 1964.
(9) JAKAB, I., 'An electrical method for the optimum damping of mechanical transducers' (in German). *Revue de Mécanique Appliquée* (Bucharest) **7**, 6, 1962.
(10) DUMITRESCU, LUCIAN Z., 'The development and use of capacitive pressure transducers for aerodynamic research.' Institute of Fluid Mechanics Report, 1964.
(11) RUDINGER, G., *Wave diagrams for nonsteady flow in ducts*. D. Van Nostrand Co., Inc. New York, 1955.

DISCUSSION

L. H. Ohman (National Aeronautical Establishment/N.R.C., Ottawa, Canada): Your oscillograph records show a pronounced high-frequency modulation. To what do you attribute these?

Dr. Dumitrescu: On some oscillograms (especially in Figs. 10, 11 and 16(*a*) a high-frequency oscillation is superposed on the pressure variation; its peak-to-peak amplitude is about 1·5% of the main signal. This phenomenon has already been observed and some special experiments have been carried out to find an explanation. Our pressure pick-ups are diaphragm-type capacitive transducers; their natural ringing frequency (of about 50 Kc/s) is damped by means of a special electrical correction circuit, individually adjusted for each pick-up to produce just the critical damping (*see* ref. 9). However, when the pick-up diaphragm is submitted to a step pressure input (produced by the head-on arrival of a shock wave), the higher harmonics of the diaphragm oscillation frequency are also excited. The first of these to give a capacity variation is the second harmonic, having in the case of our pick-ups a frequency of about 150 Kc/s; this is seen in the pictures and has been put into better evidence by special experiments. When the pressure rise is more gradual, the harmonics are not excited, and the signal is smooth (*see* Fig. 16(*b*)). Although means can be found to render the harmonics invisible on the oscillograms, these have certain disadvantages in that they introduce distortions and have not been used, since the oscillation amplitude is small and does not impair the quality of the pictures. It should be remarked that such secondary effects are showing up in our oscillograms due precisely to their high quality and to the absence of other distortions and perturbations which enables us to use the pick-ups for displaying pressure variations up to near their natural frequency.

J. L. Stollery (Aero. Dept., Imperial College, London S.W. 7., England): Would the author care to amplify his remarks about the complex wave pattern set up in a sharp bend (Fig. 13). In particular, could he differentiate between the two types of wave and say how they originate?

Dr. Dumitrescu: When the shock wave reaches the corner of the duct, first, a diffraction process similar to that shown in Fig. 4 is initiated. In this manner, a shock wave is propagated downstream, and a rarefaction (shown in Fig. 13 by a double line) is swept upstream. The process is complicated further by reflections and diffractions of the transmitted waves on the walls. The transmitted and reflected rarefaction waves, however, have the tendency to spread in width while travelling along the tube, and so become invisible on the shadowgraph. The successive reflections of the shock wave are, however, clearly visible in the picture. When the shock wave, first reflected at the outer wall of the bend, reaches again the inner corner, a second diffraction process is initiated (which has been shown also by double lines); a shock is transmitted upstream and a rarefaction travels downstream. These waves are later undergoing further reflections on the corner walls, and so on. Each time a reflected shock reaches the inner corner, a new diffraction process begins. However, the latter stages of the interactions are somewhat distorted by the presence of the corner vortex, which breaks down and is slowly swept downstream. Also, the waves become progressively weaker, until equilibrium is reached.

Dr. E. W. E. Rogers (Aero Division, N.P.L., Teddington, Middx, England): Dr. Dumitrescu has presented an interesting account of his work and shown the ability of a fairly simple theory, based on the assumption of weak shock waves, to predict the development of the shock pattern. For strong shock waves, a theoretical analysis would seem to be much more difficult; perhaps he would tell us how he proposes to tackle this aspect of his future research programme? Also, perhaps Dr. Dumitrescu could comment on the effect that the wall boundary layers, induced behind the incident shock, have on the developing shock pattern. For example, these might pose serious difficulties when the reflected shock waves are strong enough to cause flow separation.

Dr. Dumitrescu: (1) The main difficulty, in the case of strong shock waves, seems to be the fact that, as the flow velocity becomes also high, the time scales of the wave-propagation and wake-formation processes will become comparable, and the two phenomena will cease to be separable. However, preliminary tests, now being made in our laboratory, show that, at least for certain obstacle shapes, the vortices generated at the obstacle corners do not much disturb the wave pattern, so that the motion still remains self-similar, in the first phase. Therefore, the time variable can be eliminated; but the

resulting equations cannot be linearised, and a finite-difference scheme has to be used.

(2) The shock-tube boundary layer should exert its influence on the flow only late in the development of the flow, when the waves diffracted from the obstacle are reflected at the tube walls. Such circumstances have been avoided in our experiments, and our opinion is that they can be avoided also in the case of strong shocks, by using models of appropriate size.